Daclatasvir, an Antiviral Drug, Downregulates Tribbles 2 Pseudokinase and Resensitizes Enzalutamide-Resistant Prostate Cancer Cells

Jitender Monga[1,2], Frederick Valeriote[2], Clara Hwang[2], Shirish Gadgeel[2], and Jagadananda Ghosh[1,2]

ABSTRACT

FDA-approved enzalutamide is commonly prescribed to reduce growth of advanced prostate cancer by blocking androgen receptor function. However, enzalutamide-resistant prostate cancer (ERPC) invariably develops which progresses to metastatic, lethal disease. Management of ERPC poses special problem not only because available therapeutic regimens cannot effectively kill ERPC cells but also due to their propensity to invade large bones. Moreover, molecular mechanism(s) behind enzalutamide resistance is not properly understood, which is delaying development of newer agents. We found that the pseudokinase, Tribbles 2 (TRIB2), is overexpressed in ERPC cells and plays critical role in their survival. Forced overexpression of TRIB2 enhances prostate cancer cell growth and confers resistance to physiologic doses of enzalutamide, suggesting that TRIB2 plays an important role in the development and progression of ERPC. Though TRIB2 has emerged as an excellent molecular target for ERPC, suitable inhibitors are not commercially available for effective targeting. By designing a luciferase-tagged TRIB2 fusion protein-based assay system, we screened a library of about 1,600 compounds and found that daclatasvir (DCV), an antiviral drug, effectively inhibits TRIB2-luciferase. We also found that DCV degrades TRIB2 proteins by direct binding and resensitizes ERPC cells to enzalutamide treatment. Moreover, DCV at lower, sublethal doses synergize with enzalutamide to decrease the viability and induce apoptosis in prostate cancer cells. Because DCV is already approved by the FDA and well tolerated in humans, based on our findings, it appears that DCV is a promising new agent for development of an effective therapy for advanced, enzalutamide-resistant, lethal prostate cancer.

Introduction

About 271,000 men are diagnosed with prostate cancer of which ~30,000 die every year, which makes it the most common form of malignancy and second leading cause of cancer-related deaths in American men (1). Advanced prostate cancer is treated with androgen-deprivation therapy though castration-resistant prostate cancer (CRPC) invariably develops. CRPC is commonly treated with second-generation androgen blockers, such as enzalutamide, which directly binds and inhibits the androgen receptor (AR) function (2–7). Though enzalutamide extends lifespan of patients with castration-resistant disease, which highlights the benefit of targeting the AR axis, enzalutamide-resistant prostate cancer (ERPC) invariably develops (8–10). Currently, ERPC is not curable because available chemotherapeutic regimen cannot effectively kill ERPC cells, and this problem is amplified by the lack of proper molecular understanding to develop targeted therapies for ERPC. Failure of available chemotherapeutic regimen to effectively eliminate ERPC cells eventually leads to widespread tumor metastasis and causes excruciating pain and suffering. Thus, there is an urgent need to develop new target-based agents and strategies to overcome prostate cancer lethality, inflicted largely by the development of advanced diseases which are resistant to second-generation antiandrogens, such as enzalutamide.

To better understand the ERPC phenotype, we developed an *in vitro* model by chronically treating human LNCaP prostate cancer cells with gradually increasing doses of enzalutamide (up to 30 μmol/L) to mimic the clinical conditions in patients undergoing long-term enzalutamide therapy (11–13). Comprehensive gene expression analysis of the resultant cells revealed that Tribbles 2 (TRIB2) is overexpressed in the enzalutamide-resistant cells compared with parental enzalutamide sensitive cells. Overexpression of TRIB2 was also found in enzalutamide treated patient prostate tumors. Moreover, it was observed that forced overexpression of TRIB2 confers enzalutamide resistance, and inhibition of TRIB2 resensitizes and kills ERPC cells via apoptosis, suggesting that TRIB2 is a suitable target for development of a new therapy for ERPC (14). TRIB2 was originally discovered in *Drosophila* as a regulator of morphogenesis (15). Later, an association of TRIB2 was found with a range of cancers (16–18). TRIB2 is oncogenic and plays an active role in cancer aggressiveness and drug resistance (19–24). However, because of its nonenzymatic nature and absence of manageable deep pocket(s), specific targeting of TRIB2 by blocking its protein–protein interactions is extremely difficult. Thus, in spite of being recognized as a *bona fide* promoter of therapeutic resistance in prostate cancer, TRIB2 remains as an elusive molecular target for developing strategies to overcome enzalutamide resistance.

The main hurdle to develop agents to inhibit TRIB2 is the lack of a quick and easy assay procedure to effectively screen large number of compounds. Because TRIB2 is not an enzyme, its activity cannot be analyzed by measuring the rate of substrate conversion and/or product formation. To overcome this problem, we designed a new assay system to measure the active/stable state of TRIB2 protein. We made a TRIB2-luciferase gene construct by combining the full-length human TRIB2 gene with the luciferase gene from *Renilla reniformis*. Destabilization of the three-dimensional conformation of the resultant TRIB2-Luc fusion protein can deliver reportable outcomes via alteration in the enzymatic activity of luciferase. A second screen was designed to eliminate compounds that affect the activity

[1]Department of Urology, Vattikuti Urology Institute, Henry Ford Health System, Detroit, Michigan. [2]Henry Ford Cancer Institute, Henry Ford Health System, Detroit, Michigan.

Corresponding Author: Jagadananda Ghosh, Department of Urology, Henry Ford Health System, 1 Ford Place, 2D, Detroit, MI 48202. Phone: 313-433-2566; Fax: 313-874-4324; E-mail: jghosh1@hfhs.org

Mol Cancer Ther 2023;XX:XX–XX

doi: 10.1158/1535-7163.MCT-21-1002

of free luciferase. Using this dual luciferase assay system, we screened a library of ∼1,600 FDA-approved compounds and found that daclatasvir (DCV), an antiviral drug (25–30), strongly inhibits the TRIB2-luciferase activity. It was also found that though DCV inhibits the activity of TRIB2-luciferase fusion protein, it does not inhibit the free luciferase activity when TRIB2 is not attached. Thermal shift assay (TSA) revealed that DCV decreases the half-maximal melting temperature (*Tm*) of pure TRIB2 protein, which suggested that DCV may directly bind and destabilize the TRIB2 protein for enhanced degradation. Indeed, we found that DCV downregulates TRIB2 protein level and resensitizes a range of enzalutamide-resistant, aggressive prostate cancer cells. Thus, our dual luciferase-based assay system (involving primary screen and a counter-screen) emerges as an effective way to identify potential TRIB2-targeting agents using simple gene transfected cell lines in culture towards developing a new therapy for aggressive, drug-resistant cancers, such as ERPC.

Materials and Methods

Cell culture and reagents

LNCaP, PCa-2B, and LAPC4 human prostate cancer cells and human foreskin fibroblasts (HFF) were purchased from ATCC (Manassas, VA). The enzalutamide-resistant cells (ERPC cells) were generated by exposing human prostate cancer cells to an increasing concentration of enzalutamide over 6 months. Cells were grown either in RPMI1640 (Invitrogen, Carlsbad, CA) or HPC1 (AthenaES, Baltimore, MD). All the media were supplemented with 10% FBS and antibiotics. ERPC cells were maintained in the presence of enzalutamide (30 μmol/L). The final dose (30 μmol/L) was chosen to mimic the human plasma concentration of enzalutamide (16 μg/mL or ∼34 μmol/L; mol. wt. 465) reached upon three months of treatment with enzalutamide (Xtandi) at 160 mg/day (12, 13). The cell lines morphology was monitored routinely, and the cells were routinely tested for mycoplasma using PCR mycoplasma detection kit (Catalog no. J66117; Alfa Aesar, Tewksbury, MA).

Cell viability assay

Cell viability was measured by MTS/PES One Solution Cell Titer Assay (Promega Corp, Madison, WI) as described before (31, 32).

Microscopy

Cells (∼300,000) were plated overnight in RPMI1640 supplemented with 10% FBS onto 60-mm diameter tissue culture plates (Falcon) and allowed to grow for 48 hours. On the day of experiment, the spent culture medium was replaced with 2 mL fresh RPMI medium and the cells were treated with inhibitors. Control cells were treated with solvent (DMSO). Photographs were taken with a Nikon digital camera attached to a LEICA microscope at ×400. Image acquisition and data processing were done with a Dell computer attached to the microscope using Q-Capture 7 software.

Western blot

Cells (∼300,000) were plated in 60-mm diameter plates and allowed to grow for 48 hours. The old medium was then replaced with 2 mL fresh RPMI medium and then the cells were treated with inhibitors. After treatment, cells were harvested, washed, and lysed in lysis buffer (50 mmol/L HEPES buffer, pH 7.4, 150 mmol/L NaCl, 1 mmol/L EDTA, 1 mmol/L orthovanadate, 10 mmol/L sodium pyrophosphate, 10 mmol/L sodium fluoride, 1% NP-40, and a cocktail of protease inhibitors). Proteins were separated by 12% SDS-PAGE and transferred to nitrocellulose membranes. Membranes were blocked with 5% nonfat-milk solution and blotted with appropriate primary antibody followed by peroxidase-labeled secondary antibody. Bands were visualized by enhanced chemiluminescence detection kit from Pierce Biotech (Rockford, IL). To be accepted as valid, protein blots were analyzed at least in two independent experiments showing similar results. Antibodies against TRIB2, JNK (p), pAKT, FOXO3, and pH2A.X were from Cell Signaling Technology. Survivin antibody was purchased from R and D Systems (Minneapolis, MN), and antibodies against, Bcl-xL, cyclin D1, ATF3, caspase-3, and GAPDH were from Santa Cruz Biotechnology (Santa Cruz, CA). Ki-67 antibody was purchased from Sigma Chemical CO (St. Louis, MO).

DNA degradation assay

Cells (∼300,000) were plated in 60-mm diameter plates and allowed to grow for 48 hours. The old medium was then replaced with 2-mL fresh RPMI medium and then the cells were treated with inhibitors for 24 hours. Drug-treated and control cells were lysed in lysis buffer for 60 minutes at 4°C and aliquots of lysates were used for measuring DNA degradation to nucleosomal fragments using an ELISA kit from Roche (St. Louis, MO) as reported before (32).

Invasion assay

In vitro invasion assay was done using Matrigel-coated Boyden transwell chambers from BD Biosciences. Transwells were soaked in 50-μL serum-free medium for 30 minutes at room temperature and then ∼40,000 cells (in RPMI medium containing 0.1% BSA) were placed into the upper chambers. These chambers were then placed in 24 well plate (one per well) on top of 500 μL RPMI medium containing 3% FBS as chemoattractant. Inhibitors were added directly to the medium and mixed. Then the cells were incubated at 37°C in the CO_2 incubator for 16 hours. Non-invaded cells along with Matrigel in the upper chambers were scraped with a cotton tipped applicator and then the membranes were fixed in methanol, stained with 0.025% crystal violet, and observed under a Leica microscope at ×200.

Soft agar colony formation assay

Cells (10,000 per well in 6-well plates) were plated in 0.3% soft agar on top of a base layer of 0.6% agar. The cells were treated with doses of DCV, and the plates were incubated at 37°C for 3 weeks in the CO_2 incubator. Cells were given fresh media and drug every fourth day. At the end of incubation period, colonies were stained with 0.025% crystal violet, and pictures of colonies were taken with a Nikon digital camera at ×200 (31–35).

TSA

TSAs were performed using an Applied Biosystems QuantStudio 6 Flex Real-Time PCR instrument following the Protein Thermal Shift Dye Kit protocol (Applied Biosystems). Pure TRIB2 protein was diluted in protein thermal shift buffer to a concentration of 0.5 μmol/L and then incubated with the DCV (2 μmol/L) in a total reaction volume of 20 μL. The SYPRO Orange was used as a fluorescence probe.

TRIB2 modeling and DCV docking

The homology model of human TRIB2 (UniProt ID: Q92519) was built with Swiss-Model. The chemical structure of DCV (CID 25154714) was retrieved from PubChem. The ligand (DCV) was docked to the TRIB2 model with AutoDock Vina using PyRx platform.

Search space was defined as centers X = 7.6566, Y = 30.1191, and Z = 186.2056 and the dimensions (Å) X = 48.1519, Y = 63.3073, and Z = 40.9325. The docked complex was visualized using PyMOL and BIOVIA discovery studio molecular visualization tools.

Drug combination assay

The cells were co-treated with the defined concentrations of enzalutamide and DCV and the cytotoxic effects of the individual drugs and its combinations were measured using MTS assay. The drugs synergy was determined using SynergyFinder 2.0 software (36). The synergistic interaction between drugs has a score greater than +10; an additive interaction has a score between −10 to +10; and an antagonistic interaction has a score of less than −10. Deviations between observed and expected responses with positive (red areas) and negative δ-values (green areas) indicate synergy and antagonism, respectively.

In vivo tumor xenografts

Animal studies were approved by the Institutional Animal Care and Use Committee and performed according to the institutional guidelines for animal care and handling. To analyze the effect of DCV on enzalutamide-resistant prostate tumor growth, exponentially growing LNCaP-ENR cells (3×10^6 cells/mouse in 50% Matrigel in PBS) were subcutaneously injected into the right flanks of 7-week-old male athymic nude mice ($n = 4$). When the tumors grew to approximately 100 mm^3, mice were randomized and treated with vehicle or DCV (30 mg/kg/day) or enzalutamide (30 mg/kg/day) orally for 4 weeks. Tumor size and mice body weights were measured once per week. Tumor growth was monitored by measuring volumes using a digital slide calipers. Tumor volumes were calculated by the formula $TV = a \times (b)^2/2$.

Statistical analysis

Statistical significance was assessed by two-way ANOVA or the two-tailed Student *t* test and a value of <0.05 was defined as significant. Results are expressed as the mean ± SEM and are described in each figure legend when applied.

Data availability

The data generated in this study are available within the article.

Results

High-throughput screening identifies DCV as a novel agent to downregulate TRIB2

The amino acid sequence in TRIB2 protein bears similarity to a standard kinase and binds ATP, but it lacks a strong kinase activity (pseudokinase). Thus, we designed an assay system by combining full-length human TRIB2 gene with the luciferase gene from Renilla to make a fusion construct. After analyzing a range of established cancer as well as non-cancer cell lines we found that the HFFs do not express detectable TRIB2 protein. Thus, to avoid the interference from endogenous TRIB2 and regulators of TRIB2, we selected HFF cells for transfection of the luciferase tagged TRIB2 gene construct. Cells were selected for overexpression of the fusion gene by two rounds of drug (G418) selection. The resultant cells (HFF-TRIB2-Luc) showed strong luciferase activity and a protein product of the size of ∼72 kDa, suggesting that the fusion construct translates into a functional protein product inside the cells. Using the HFF-TRIB2-Luc cells we screened a library of about 1,600 FDA approved compounds (# HY-L022) purchased from MedChem Express (Monmouth Junction, NJ). Drug effects were tested in 96-well tissue culture plates following a standardized 24-hour assay protocol (**Fig. 1A**). Our assays revealed that about 1% of the compounds can inhibit TRIB2-Luc activity by 70% or more. Interestingly, we found that DCV, an antiviral drug downregulates the luciferase activity in the first screen by 74% (**Fig. 1B** and **C**). Moreover, we found that DCV does not inhibit control luciferase activity in the second screen, suggesting that the effect of DCV may be because of its interaction with TRIB2. Some other antiviral compounds were also tested, such as Ledipasvir (LDV), darunavir, and dolutegravir which were completely ineffective to inhibit TRIB2-luciferase activity in the same experimental system, indicating that a critical structural component/configuration is the key to inhibit TRIB2 rather than a generalized antiviral property of the compounds. From the effects of unknown compounds in the TRIB2-Luciferase fusion protein-based assay system, it appears that this screening process is effective to identify potential hits which can be further tested in cell culture assays to validate TRIB2-targeting compounds based on potency and cancer selectivity.

DCV directly binds and destabilizes TRIB2 protein

Though DCV showed selective effect on TRIB2 based on luciferase assays, whether it directly binds with TRIB2 was not clear. To address this, we used a TSA of pure TRIB2 protein for analysis of drug–protein interactions. The TSA curve of purified recombinant human TRIB2 protein showed that treatment with DCV shifts the melting curve to the left (**Fig. 2A**). The Tm (midpoint of temperature for melting) was found to be decreased from 41°C to 37°C, suggesting destabilization of the TRIB2 protein by DCV. This finding also implicates that DCV may change the ubiquitination state of TRIB2 protein inside the cell towards enhanced degradation involving proteasome activity. The Swiss-Prot computer modeling using complete amino acid sequence of the human TRIB2 protein revealed that six amino acids **(Glu-71, Ser-100, Ser-133, Glu-194, Glu-197**, and **Asp-198)** interact with the DCV molecule (**Fig. 2B–E**). The computer model also suggested that DCV non-covalently binds and destabilizes TRIB2 protein (**Fig. 2D**).

DCV downregulates TRIB2 protein level via proteasomal degradation

We found that DCV efficiently downregulates TRIB2 protein level and decreases the viability of ERPC cells (**Fig. 3A–D**). In our assays, we found that DCV inhibits TRIB2 at micromolar doses, but LDV (#7), another antiviral drug, neither downregulates TRIB2 nor kills ERPC cells, suggesting that the selective effect of DCV against TRIB2 protein is due its structural component(s) not present in LDV. To verify the effects of DCV we analyzed its effect on TRIB2 downstream markers and found that DCV inhibits the protein levels of pAKT, Bcl-xL, and survivin, and increased the level of the tumor suppressor, FOXO3 (**Fig. 3E**). We also found that DCV enhances degradation of TRIB2 protein, and this process involves proteasome activity (**Fig. 3F** and **G**). DCV strongly inhibits the *in vitro* invasion through extracellular matrix and the colony-forming abilities of LNCaP-ENR cells (**Fig. 3H** and **I**). Thus, DCV as an inhibitor of TRIB2 can stop the invasion and recolonization of advanced cancer phenotype which are characteristic features of ERPC cells. Altogether, our findings indicate that the antiviral drug DCV is a novel inhibitor of TRIB2 and can be effective against a range of cancers which overexpress the TRIB2 pseudokinase.

DCV kills ERPC cells by inducing apoptosis

We found that DCV effectively reduced the viability of ERPC cells (**Fig. 4A** and **B**). DCV (Daklinza) is an FDA-approved drug for

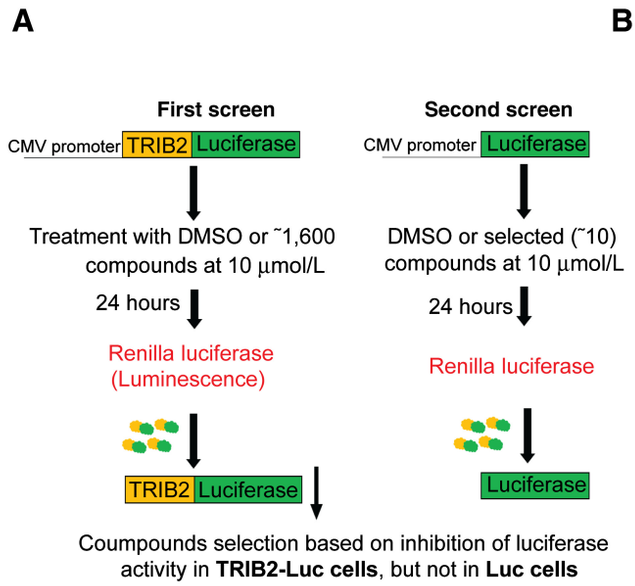

B

Compound	Luciferase activity (%)	Compound	Luciferase activity (%)
Dichlorphrnamide	100	Darunavir	93
Ranolazine	100	Niraparib tosylate	93
6-Acetamidohexanoic	100	Clofibric acid	87
Alcaftadine	100	Ajamaline	93
Temsirolmus	94	Sulfamethizole	94
Oxaceprol	100	Fimasartan	88
Mianserin	55	Anagrelide	92
Dolutegravir	100	Nadifloxacin	96
Nilotinib	99	Ponatinib	42
Efonidipine	98	Valnemulin	83
Dirithromycin	100	Mozavaptan	86
Clebopride	100	Dipyridamole	98
Ibudilast	85	Lansoprazole	78
Ramelteon	100	Atropine	67
Chlormerazanoine	100	Olmesartan	80
Famotidine	100	Estrone	82
Busulfan	100	Hydroxyfasudil	46
Epalrestat	53	Sulfaguanidine	84
Ornipressin	27	Prazosin	49
Ampiroxicam	28	Tigecycline	63
Droperidol	100	Doxorubicin	28
Nilvadipine	89	Ledipasvir	100
Triamterene	100	Levocarnitine	84
Methacholine	99	Sulfadiazine	70
Doxycycline	91	Guanfacine	100
Alprenolol	91	Tavaborole	75
Niclosamide	62	Isosorbide	91
Irinotecan	85	Betamipron	87
Fenofibrate	92	Udenafil	100
Ethambutol	98	Milnacipran	85
Gadodiamide	89	Carbidopa	92
Teniposide	70	Imipramine	86
Vincamine	80	Telotristat etiprate	94
Pemirolast	88	Trimetazidine	100
Cromolyn	93	Ronidazole	100
5-Aminosalicyclic acid	84	Malathion	91
Tamibarotene	100	Danofloxacin	81
Dapoxetine	88	Azasetron	100
Telbivudine	91	Plerixafor	93
Mexiletine	86	Meloxicam	100
Noscapine	100	Tegafur	100
Efavirenz	89	Terconazole	82
Penciclovir	97	Dabrafenib	72
Tebipenem pivoxil	100	Triamcinolone	72
Venetoclax	184	Vorapaxar	59
Chlorambucil	96	Proparacaine	88
Resperine	91	Erlotinib	50
Clarithromycin	97	Daclatasvir	28
Etomidate	100	Pyridostigmine	76
Dexrazoxane	100	Fingolimod	80
Paroxetine	93	Minaprine	79
Penfluridol	71	Ticarcillin	87
Fluocinonide	78	Budesonide	83

C

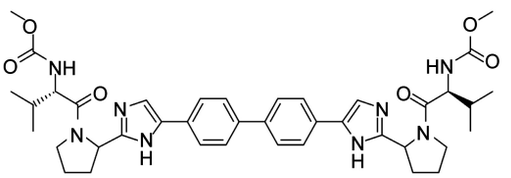

Figure 1.

High-throughput screening identifies DCV as TRIB2 degrader. **A,** Schematic representation of the TRIB2-Luciferase fusion protein-based assay system. **B,** Effects of a representative set of 106 FDA-approved compounds on Trib2-Luciferase fusion construct-transfected HFF cells are shown here. Cells were plated in 96 well plates and treated with the compounds (10 µmol/L) for 24 hours in the CO_2 incubator. Luciferase activity was measured using a kit from Promega Corp (Madison, WI). For further development selected compounds were counter-screened with control luciferase-transfected HFF cells. Note: DCV showed more than 70% inhibition of TRIB2-luciferase activity in 24 hours and passed the counter-screen tests. **C,** Chemical structure of DCV, a biphenyl-carbamate.

hepatitis C virus (HCV) owned by Bristol-Myers Squibb. It belongs to the class of direct-acting antivirals (DAA) and is known to inhibit the hepatitis C viral nonstructural protein 5A (NS5A) which is important for the replication of the virus (37–41). Here, our experiments with cancer cells revealed that DCV triggers degradation of TRIB2 protein and decreases the viability of ERPC cells, which opened a new avenue for its repurposing against TRIB2-overexpessing cancers, such as ERPC. We also found that DCV treatment reduced the viability of AR-negative and AR-mutated aggressive prostate cancer cells (Supplementary Fig. S1 and S2). DCV treatment resulted in G_1-phase arrest in ERPC cells accompanied by a decrease of the cell population in the S phase (**Fig. 4C**). To understand how DCV kills ERPC cells, we observed significant induction of apoptosis in ERPC cells upon DCV treatment, as measured by Annexin V staining by Flow Cytometry (**Fig. 4D**), and ELISA-based DNA fragmentation (**Fig. 4E**) analysis. Characteristic cleavage of PARP which is an indicator of apoptosis was also observed in DCV treated ERPC cells (**Fig. 4F**). We also found that DCV decreased the protein level of cell proliferation regulator, cyclin D1, and increased the level of proapoptotic protein, ATF3 in ERPC cells (**Fig. 4F**). DCV also induced phosphorylation of the H2A.X at Serine139 (**Fig. 4F**), suggesting induction of DNA damage in ERPC cells. To explore the underlying mechanism of DCV-induced apoptosis in ERPC cells, we analyzed effect of DCV on c-Jun N-terminal kinases (c-JNK) which play a critical role in apoptotic pathways (36). We found that DCV triggers rapid and robust activation of the c-JNK in a dose-dependent manner in ERPC cells (**Fig. 4G**). Both caspase dependent and caspase-independent apoptotic cell death processes are known (31, 32, 34). Here, we observed that treatment with DCV induces activation of caspase-3 in LNCaP-ENR cells (**Fig. 4H**). Moreover, it was found that the DCV treatment-induced apoptosis in ERPC is inhibited when the cells were pretreated with a caspase inhibitor, Z-VAD-FMK, suggesting that the DCV-induced apoptosis in ERPC cells is caspase-dependent (**Fig. 4I**). Interestingly, cells treated with LDV (also an inhibitor of HCV) did not show any signs of apoptotic features (**Fig. 4E**), suggesting that the effect of DCV to induce apoptosis in ERPC cells is selective. Next, we found that DCV remarkably blocked the soft agar colony formation (an *in vitro* test for tumorigenicity) by ERPC cells (**Fig. 4J**). Complete inhibition of colony formation by ERPC cells signifies that DCV can penetrate to overcome the resistance due to compactness and hypoxic environment at the core of the lumpy mass of ERPC cells. Thus, a superior *in vivo* effectiveness of DCV against ERPC can be expected.

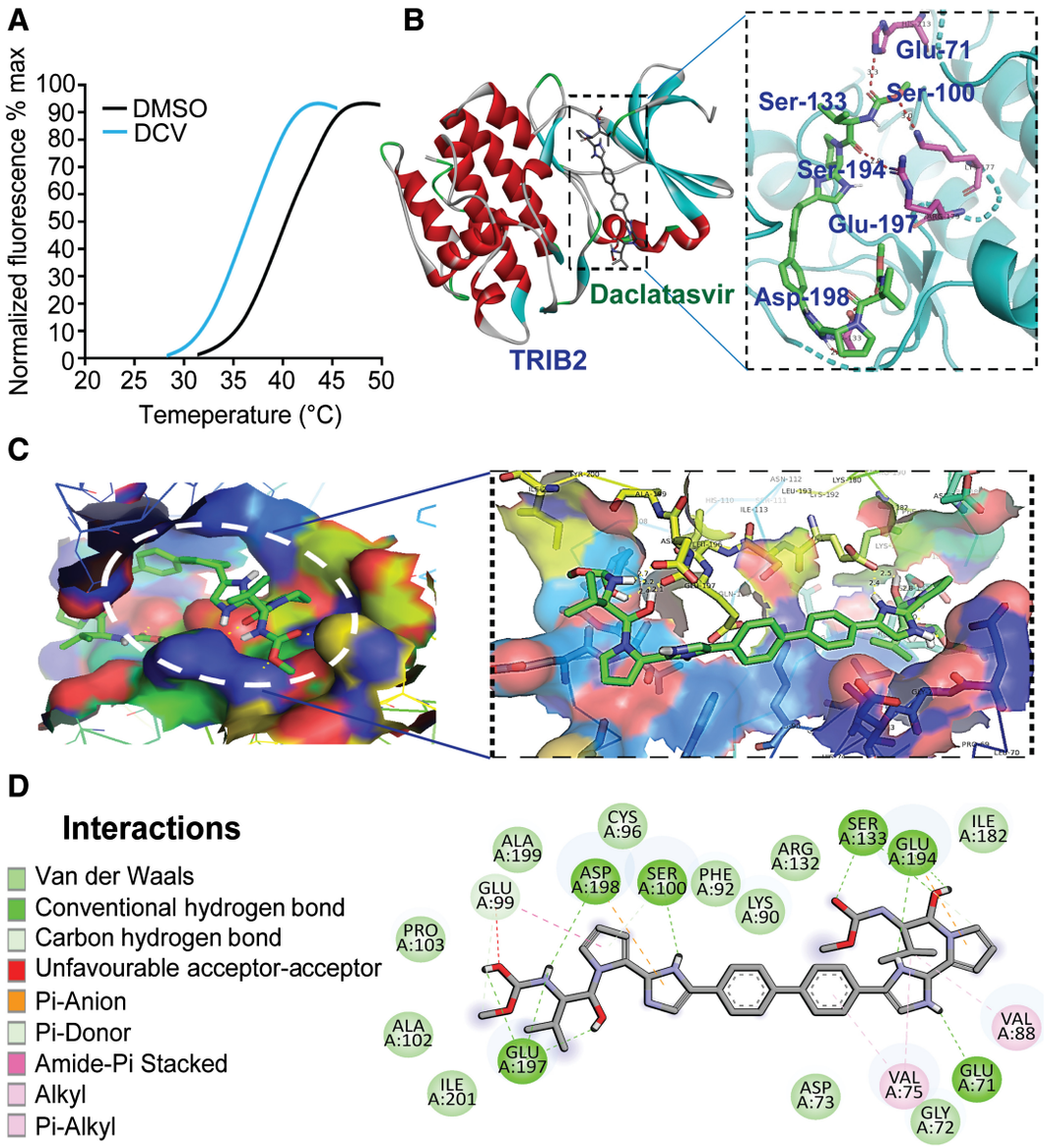
A
Normalized fluorescence % max
100
90
80
70
60
50
40
30
20
10
0
DMSO
DCV
20 25 30 35 40 45 50
Temeperature (°C)
B
Glu-71
Ser-133
Ser-100
Ser-194
Glu-197
Asp-198
Daclatasvir
TRIB2
C
D
Interactions
Van der Waals
Conventional hydrogen bond
Carbon hydrogen bond
Unfavourable acceptor-acceptor
Pi-Anion
Pi-Donor
Amide-Pi Stacked
Alkyl
Pi-Alkyl
CYS A:96
ALA A:199
ASP A:198
SER A:100
PHE A:92
ARG A:132
SER A:133
GLU A:194
ILE A:182
GLU A:99
LYS A:90
PRO A:103
ALA A:102
GLU A:197
ILE A:201
ASP A:73
VAL A:75
GLY A:72
GLU A:71
VAL A:88
E
10 20 30 40 50
MNIHRSTPIT IARYGRSRNK TQDFEELSSI RSAEPSQSFS PNLGSPSPPE
60 70 80 90 100
TPNLSHCVSC IGKYLLLEPL EGDHVFRAVH LHSGEELVCK VFDISCYQES
110 120 130 140 150
LAPCFCLSAH SNINQITEII LGETKAYUVFF ERSYGDMHSF VRTCKKLREE
160 170 180 190 200
EAARLFYQIA SAVAHCHDGG LVLRDLKLRK FIFKDEERTR VKLESLEDAY
210 220 230 240 250
ILRGDDDSLS DKHGCPAYVS PEILNTSGSY SGKAADVWSLGVMLYTMLVG
260 270 280 290 300
RYPFHDIEPS SLFSKIRRGQ FNIPETLSPK AKCLIRSILR REPSERLTSQ
310 320 330 340
EILDHPWFST DFSVSNSAYG AKEVSDQLVP DVNMEENLDP FFN

DCV inhibits ERPC tumor growth in nude mice

To investigate the antitumor effects of DCV *in vivo*, we subcutaneously implanted LNCaP-ENR cells into the right flanks of athymic nude mice. Starting at day 11 postimplantation, the mice were treated with either vehicle or DCV for 28 days (**Fig 5A**). We found that DCV at 30 mg/kg/day (MTD of DCV: > 100 mg/kg/day) inhibits ERPC tumor growth in nude mice without any overt toxicity to animal health (**Fig. 5B** and **C**). These finding suggest that DCV is a suitable compound with excellent *in vivo* effect that effectively eliminate deadly ERPC cells towards establishing a new therapy for deadly AR therapy–resistant prostate cancer. IHC analysis of tumor tissues showed that DCV decreased the protein levels of TRIB2 *in vivo* (**Fig. 5D**). We also found that DCV-treated tumors showed strong dephosphorylation of AKT at S473 and a strong decrease in Ki-67 positive cells (**Fig. 5D**).

DCV resensitizes resistant prostate cancer cells to enzalutamide

Treatment with enzalutamide triggers overexpression of TRIB2 in prostate cancer cells (**Fig. 6A–C**). Moreover, forced overexpression of TRIB2 has been found to confer resistance to enzalutamide, suggesting that TRIB2 is a driver of the resistance mechanism to second-generation antiandrogens, such as enzalutamide (14). Because DCV effectively downregulates the protein level of TRIB2, we wanted to examine whether DCV can reverse enzalutamide resistance in prostate cancer cells via downregulation of TRIB2. We found that TRIB2—short hairpin RNA (shRNA) or DCV effectively downregulates TRIB2 protein level and resensitizes both the enzalutamide-resistant LNCaP-ENR and PCa-2B-ENR cells (**Fig. 6D–F**). Treatment with DCV showed an increase in AR protein level in ERPC cells (**Fig. 6G** and **H**), which may result from derepression of the effects of TRIB2 on AR (14). Combination of DCV and enzalutamide was found to be more effective to decrease the growth of enzalutamide-resistant prostate tumors *in vivo* (**Fig. 6I**). We also found that DCV and enzalutamide synergistically affect the viability of enzalutamide-sensitive prostate cancer cells *in vitro* (**Fig. 6J–M**). Moreover, combination of DCV and enzalutamide was also found to increase apoptosis in prostate cancer cells, over single agent treatments, as seen by the DNA fragmentation analysis (**Fig. 6N**).

Discussion

Introduction of the second-generation AR blockers (e.g., enzalutamide) is one of the most remarkable achievements that happened in the last decade for prostate cancer therapy. However, even after initial good response, enzalutamide-resistant, lethal disease invariably develops, the mechanism of which is not properly understood. To understand the molecular basis of resistance, we comprehensively analyzed clinically relevant cell culture models as well as tumor tissues and found that during the transition of prostate cancer from an androgen-dependent to an androgen-independent state, upregulation of the TRIB2 pseudokinase is a major molecular event (**Fig. 6A–C**). We also found that in contrast to the ERPC cells which express high levels of TRIB2, the expression of TRIB2 in normal, noncancer cells is undetectable. Moreover, inhibition of TRIB2 by shRNA kills ERPC cells via caspase mediated apoptosis, while the normal, non-cancer cells are not affected (14). These findings indicated that the TRIB2 oncogene plays a selective, critical role in ERPC cells, suggesting that TRIB2 is an excellent target to develop a novel approach to effectively eliminate ERPC cells via induction of apoptosis.

Though TRIB2 has emerged as a promising molecular target for androgen-independent prostate cancer, targetable small molecule agents to inhibit TRIB2 are not commercially available currently. High dose of the kinase inhibitor, afatinib, inhibits TRIB2 but it is nonselective and too toxic (16). In our blinded screening, we found that DCV strongly inhibits TRIB2-luciferase activity but does not inhibit luciferase activity in the absence of TRIB2 protein, suggesting that DCV interacts with TRIB2, rather than the luciferase itself. Interestingly, while DCV inhibits TRIB2-luciferase activity, several other antiviral compounds, such as LDV, dolutegravir, darunavir, and penciclovir were not effective, which suggests that a unique structural component in the DCV molecule is critical to inhibit TRIB2. DCV is a DAA agent and binds with hepatitis C viral nonstructural protein 5A (37–41). However, the drug–protein interactions of DCV have not been characterized yet in mammalian cells. Thus, our design of luciferase-tagged fusion protein-based assay and TSA, to screen a library of compounds to find DCV as a direct TRIB2 protein-binding inhibitor is a remarkable observation (**Figs. 1** and **2**). The orientation of DCV in the cleft region of TRIB2 molecule suggests that polar contacts are established between the ligand and the protein, and that six amino acid residues (Glu-71, Ser-100, Ser-133, Glu-194, Glu-197, and Asp-198) of TRIB2 form hydrogen bonds with DCV. The binding pocket residues of the TRIB2 take part in the hydrogen, hydrophobic, and van der Waals interactions with DCV, suggests that this interaction is non-covalent.

DCV substantially decreased the protein level of TRIB2 in ERPC cells within 24 hours, presumably due to direct interaction with the TRIB2 protein which changed its ubiquitination status and primed it for proteasomal degradation. Enhanced degradation of TRIB2 protein corresponds well with the decrease of its downstream targets, such as p-Akt, Bcl-xL, and survivin (**Fig. 3A–E**), which are known to play critical roles in pro-survival mechanisms preventing apoptosis. Furthermore, as expected, DCV treatment increased the protein level of the tumor suppressor, FOXO3-alpha. This may have happened presumably via inhibition of TRIB2 which is known to downregulate FOXO3 via activation of Akt. Our results with cycloheximide and MG132 (a proteasome inhibitor) suggest that DCV induces TRIB2 degradation via activation of the proteasomal pathway (**Fig. 3F** and **G**). Therapy-resistant cancer cells develop extraordinary ability to invade surrounding tissues, move to distant sites and recolonize to generate metastatic nodules which ends up with lethal disease. We found that DCV strongly inhibits *in vitro* Matrigel invasion and colony formation

Figure 2.

Direct interaction of DCV with Trib2 protein: **A**, TSA of pure TRIB2 protein by Differential Scanning Spectro-fluorometry showed that DCV shifts the melting curve of Trib2 to the left (*Tm* decreased), suggesting destabilization of TRIB2 protein by DCV. **B** and **C,** Molecular docking analysis of TRIB2 protein with DCV (ligand). For molecule docking, the homology model of human TRIB2 (UniProtKB ID: Q92519) was built with Swiss-Model by submitting the FASTA sequence on the server. The top-ranked model based on sequence similarity was used for the docking studies. The chemical structure of DCV (CID 25154714) was retrieved from PubChem. The ligand (DCV) was docked to the TRIB2 model with AutoDock Vina using PyRx platform. Search space was defined as centers $X = 7.6566$, $Y = 30.1191$, and $Z = 186.2056$ and the dimensions (Å) $X = 48.1519$, $Y = 63.3073$, and $Z = 40.9325$. The docked complex was visualized using PyMOL molecular visualization tool. **B,** The polar contacts established between the ligand (DCV) and the protein (TRIB2). **C,** The three-dimensional orientation of DCV in the active site of the TRIB2 protein. **D,** The binding pocket residues of the TRIB2 taking part in the hydrogen, hydrophobic, and van der Waals interactions, are highlighted. **Glu-71, Ser-100, Ser-133, Glu-194, Glu-197,** and **Asp-198** residues of the TRIB2 formed a hydrogen bond with the DCV. **E,** Amino acid sequence of TRIB2 showing residues interact with DCV.

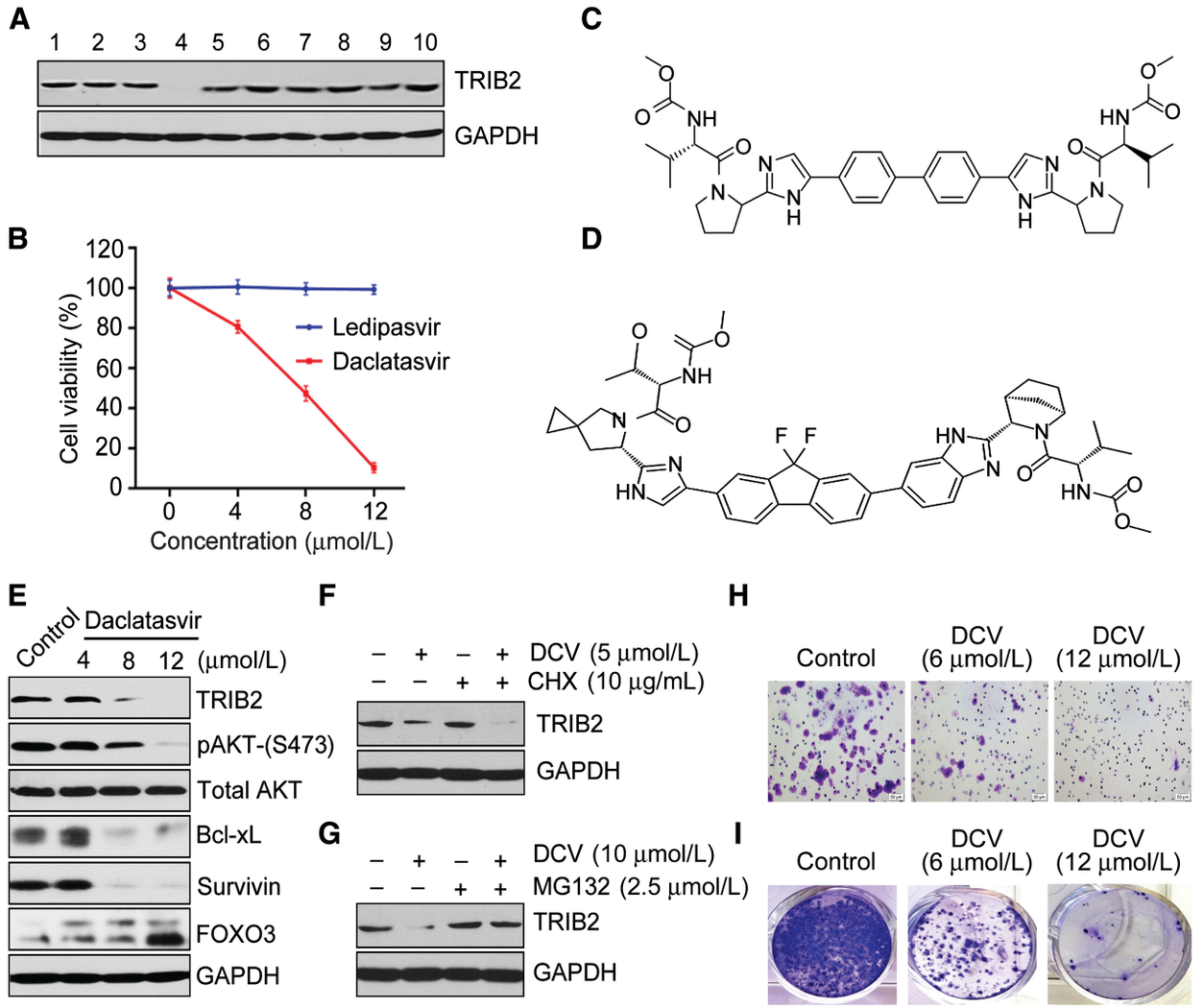

Figure 3.

Proteasomal degradation of TRIB2 by DCV. **A,** LNCaP-ENR cells were plated and treated with various drugs (at 10 μmol/L) for 24 hours and whole-cell lysate proteins were analyzed by Western blot. GAPDH was used as loading control. Lane assignment: 1 = Control; 2 = Ampiroxicam; 3 = Prazosin; 4 = DCV; 5 = Ornipressin; 6 = LDV; 7 = Lapatinib; 8 = Vorapaxar; 9 = Ponatinib; 10 = Mianserin. Note: Trib2 protein level was strongly downregulated by DCV (#4), but not by another antiviral drug LDV (#6). **B,** LNCaP-ENR cells (~3,000 cells per well) were plated in 96 well plates in complete growth medium (RPMI plus 10% FBS) and treated with varying doses of DCV or LDV. Plates were incubated for 72 hours at 37°C in the CO_2 incubator. Cell viability was measured by MTS/PES cell titer assay (Promega Corp). Note: Cell viability was effectively decreased by DCV, but not by LDV. **C,** Chemical structure of DCV (**active**) and (**D**) LDV (**inactive**). **E,** LNCaP-ENR cells were plated and treated with doses of DCV for 24 hours. Whole-cell lysate proteins were separated by SDS-PAGE and levels of TRIB2, and targets were analyzed by Western blot. **F,** Effect of DCV on degradation of TRIB2 was analyzed by treating cells with DCV with or without cycloheximide (CHX). **G,** Role of proteasome on DCV-induced degradation of TRIB2 was examined by treating cells with the chemical inhibitor, MG132. **H,** Effect of DCV on invasion was measured by using Matrigel coated Boyden invasion chambers. Chambers were soaked in RPMI medium and about 40,000 cells were placed on top of Matrigel and incubated for 16 hours in the CO_2 incubator. Invaded cells were detected by staining with crystal violet. **I,** Effect of DCV on colony formation was measured using LNCaP-ENR cells. Cells (500 per well in 6 well plates) were plated. The cells were treated with indicated doses of DCV, and the plates were incubated at 37°C for 2 weeks in the CO_2 incubator. Cells were given fresh media every fourth day. At the end of incubation period, colonies were stained with 0.025% crystal violet.

by ERPC cells (LNCaP-ENR) at sublethal doses (**Figs. 3H**, **I**, and **4J**), suggesting that the aggressive and metastatic tumor-forming abilities of ERPC cells could be effectively controlled by DCV via downregulation of TRIB2. DCV severely alters the morphology and decreases the viability of ERPC cells (**Fig. 4A** and **B**). Recently, we reported that knockdown of TRIB2 by shRNA results in strong morphologic alterations and decrease in the viability of ERPC cells (14). DCV induced morphologic changes in prostate cancer cells reminded us about involvement of apoptosis. We found that DCV enhances annexin V binding which corresponds to externalization of phosphatidylserine, a hallmark of apoptosis (**Fig. 4D**). Moreover, DCV triggers degradation of chromatin DNA to nucleosomal fragments, cleavage of PARP, upregulation of ATF3, and phosphorylation of H2A.X, confirming that DCV induces apoptosis in ERPC cells (**Fig. 4E** and **F**). Activation of the stress-activated c-JNK plays a central role in the apoptosis process (31–34). We found a robust activation of c-JNK by DCV (**Fig. 4G**). In

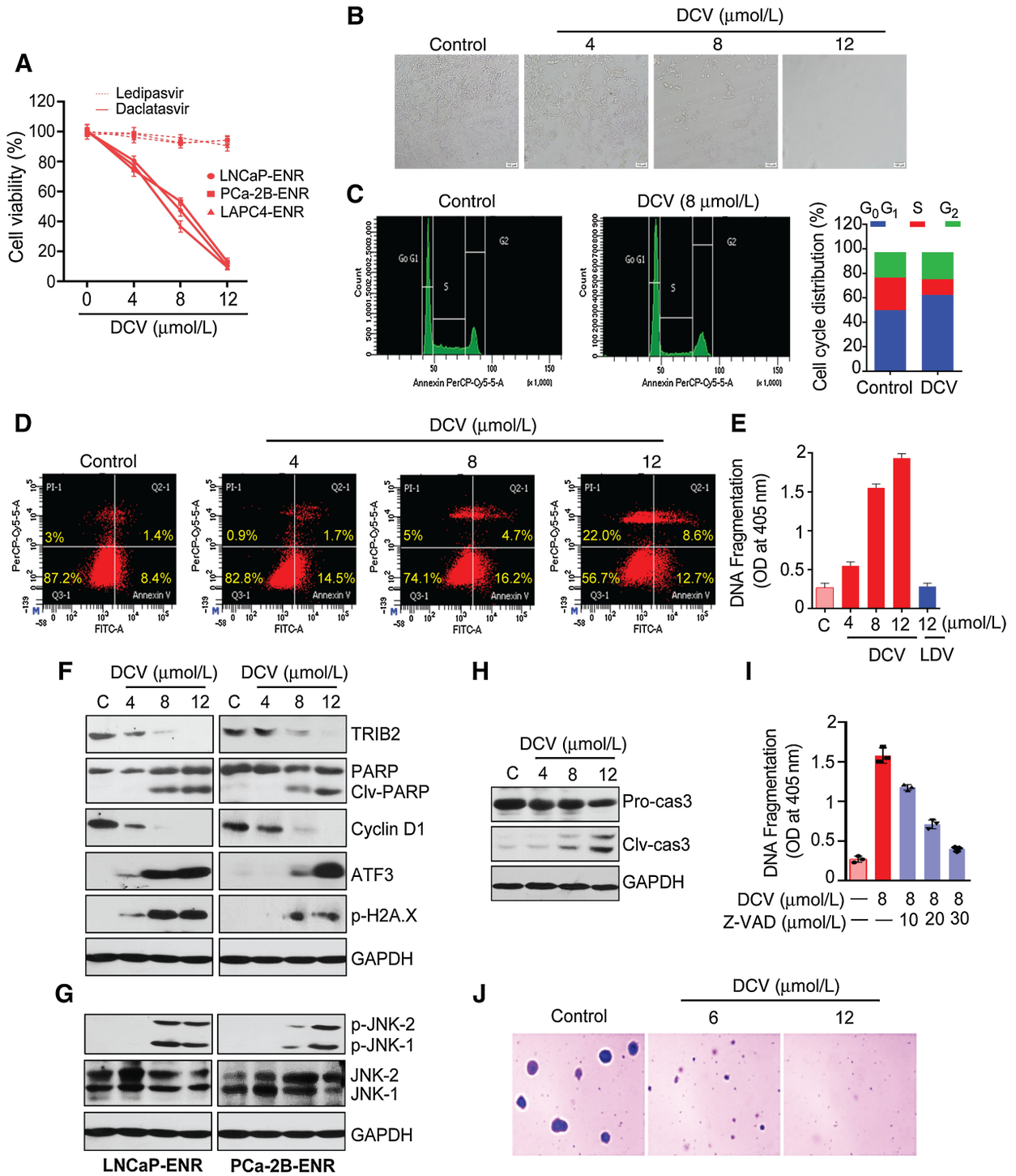

Figure 4.

DCV induces apoptosis in ERPC cells. **A,** ERPC cells were treated with indicated doses of DCV or LDV for 72 hours and cell viability was analyzed by MTS/PES assay. **B,** LNCaP-ENR cells were treated with varying doses of DCV, and the cells morphology was observed under phase contrast microscope. The cell cycle analysis (**C**) and apoptosis (**D**) were assessed by flow cytometer in LNCaP-ENR cells treated with DCV for 24 hours. **E,** Apoptotic effects of DCV were measured by DNA degradation assay. **F,** Western blot analysis showing changes in the protein levels of apoptosis, cell survival and DNA damage regulating proteins in ERPC cells treated with DCV for 24 hours. **G,** Phosphorylation/activation of c-JNK and (**H**) activation/cleavage of caspase-3 was detected in DCV treated ERPC cells by Western blot. GAPDH protein bands shown in **F** and **G** are identical as the proteins were analyzed using the same membrane. **I,** DCV induced apoptosis was inhibited by Z-VAD-FMK, a pan-caspase inhibitor in LNCaP-ENR cells. **J,** Effect of DCV on soft agar colony formation was measured using LNCaP-ENR cells. Colonies were stained with 0.025% crystal violet, and pictures of colonies were taken with a Nikon digital camera at x200. Graphs show mean ± SEM of three independent experiments.

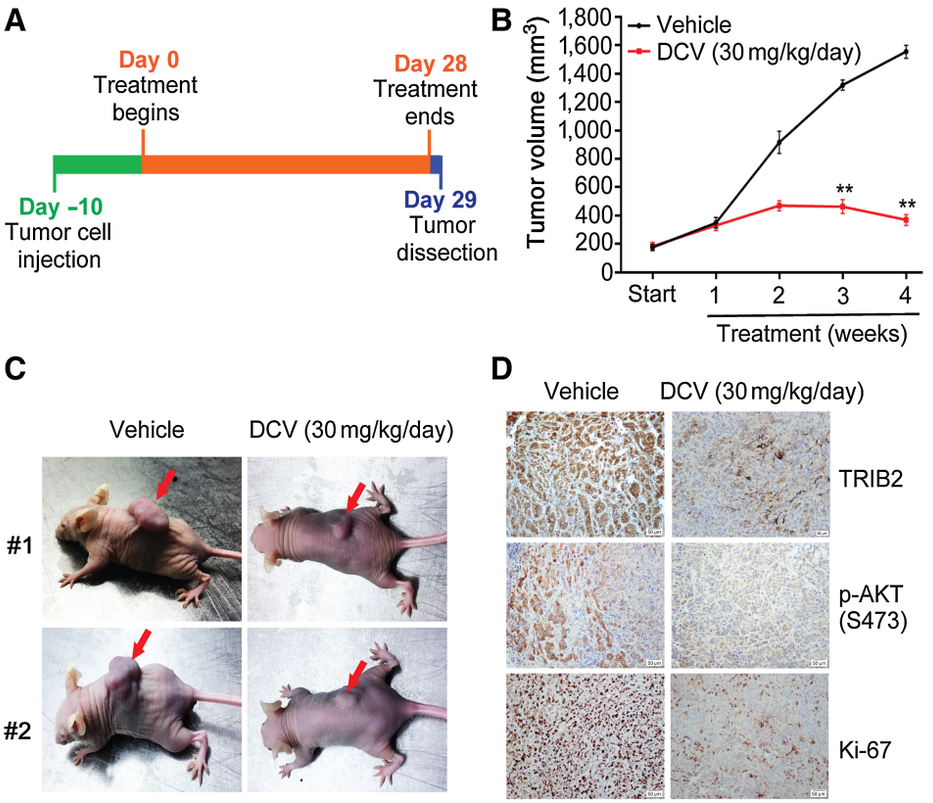

Figure 5.

DCV inhibits the growth of enzalutamide-resistant prostate tumors. **A** and **B,** BALB/c nude mice were subcutaneously injected with LNCaP-ENR cells (3×10^6 per mouse) to develop tumors and treated with 30 mg/kg/day DCV or solvent orally for 4 weeks ($n = 4$). Tumor size and mice body weights were measured once per week. Tumor volumes were calculated by the formula TV = a x $(b)^2/2$. **, $P < 0.005$. **C,** Representative control and DCV-treated mice tumors are shown. **D,** TRIB2 protein levels in control and treated mice tumors was analyzed by IHC using monoclonal anti-Trib2 antibody from Cell Signaling Technology, Danvers, MA (catalog no. 13533). The protein expression of pAKT and Ki-67 was detected in xenograft tumors by IHC. Slides were processed for IHC using Vectastain Elite Impression Kit (Vector Labs). Note: DCV was effective to decrease TRIB2 protein level as well as tumor volumes. No signs of overt toxicity (significant loss of animal body weight, or change in locomotion, food intake, skin color, diarrhea, color of urine, general viscera) was observed with DCV treatment for 4 weeks.

addition, treatment with DCV resulted in cleavage of caspase-3 and the DCV induced apoptosis was inhibited by caspase inhibitors (**Fig. 4H** and **I**). Altogether, these findings suggest that DCV kills ERPC cells via induction of caspase-dependent apoptosis.

ERPC cells are characterized by rapid growth and metastasis which quickly deteriorate the health of patients with prostate cancer, turning into a lethal phenotype. Thus, the induction of apoptotic death in ERPC cells by DCV is a significant event which may be useful to debulk tumor load. We found that DCV is effective *in vivo* to reduce ERPC tumor growth (**Fig. 5**), and that DCV sensitizes the ERPC cells back to enzalutamide, presumably via inhibition of TRIB2 (**Fig. 6D–F**). In our analysis, we found that DCV treatment upregulated AR in ERPC cells (**Fig. 6G**). We presume that this may have happened due to DCV-induced downregulation of TRIB2 and consequent derepression of the effect of TRIB2 on AR. Recently, we reported that TRIB2 effectively downregulates AR protein level in prostate cancer cells, though the exact mechanism is not fully understood yet (14). It appears that DCV apparently removes the obstacle (TRIB2), overexpression of which confers resistance to antiandrogenic therapy. These findings may have significant clinical impact in designing newer strategies to develop more effective therapies for ERPC. Our interest in ERPC stems from the fact that enzalutamide, which is prescribed post docetaxel failure, extends lifespan but no effective treatment options remain when resistance to enzalutamide develops. Currently, most of the men's lives lost due to prostate cancer is because of the development of ERPC-like advanced, aggressive cancer. Our findings may provide additional impetus to further examine DCV towards clinical development against ERPC, because DCV is already approved by the FDA and is a well-tolerated drug for human use. Thus, finding of DCV as a new TRIB2 inhibitor appears to be a highly significant observation to develop an effective and novel therapeutic strategy against aggressive, enzalutamide-resistant, lethal prostate cancer.

Lack of a suitable chemical inhibitor of TRIB2 is delaying development of a potentially new targeted therapy for ERPC. Our findings, for the first-time, document that the antiviral compound, DCV, inhibits TRIB2 and effectively kills ERPC cells. DCV (Daklinza) is an FDA-approved anti-hepatitis C viral drug, owned by the Bristol-Myers Squibb company. On the basis of the ALLY-3 randomized, multicenter, open-label, active-controlled clinical trial using 60 mg DCV (equivalent to 66 mg DCV dihydrochloride) along with 400 mg of sofosbuvir (Sovaldi) via once daily oral dose for 12 weeks in 152 patients (NCT02319031), DCV was given approval for use in HCV infection in July of 2015 (42, 43). The uptake rate of DCV is about 67% when delivered orally. In *in vivo* system, DCV stays mostly as protein bound (~99%) and metabolized mainly through liver and inhibits p-glycoprotein (44–47). Acute toxicity studies of DCV in laboratory animals demonstrated low toxicity with minimal clinical signs and no evidence of organ toxicity. The maximum non-lethal dose in mice and rat was found to be 1,000 mg/kg, and in dogs and monkeys was 150 mg/kg (Australian Government Therapeutic Goods Administration: AusPAR DCV Dihydrochloride/Daklinza, Bristol-Myers Squibb Australia Pty Ltd PM-2014–00647–1-2 Final 14 December 2015; https://www.tga.gov.au). Thus, DCV possesses excellent pharmacologic properties. However, direct effect of DCV on mammalian cells is not well studied, and its effect on cancer cells had never been addressed before. Thus, our new findings opened an opportunity for using DCV to downregulate TRIB2 protein involving proteasomes and repurpose DCV to develop a new therapy for aggressive, lethal cancers, such as ERPC.

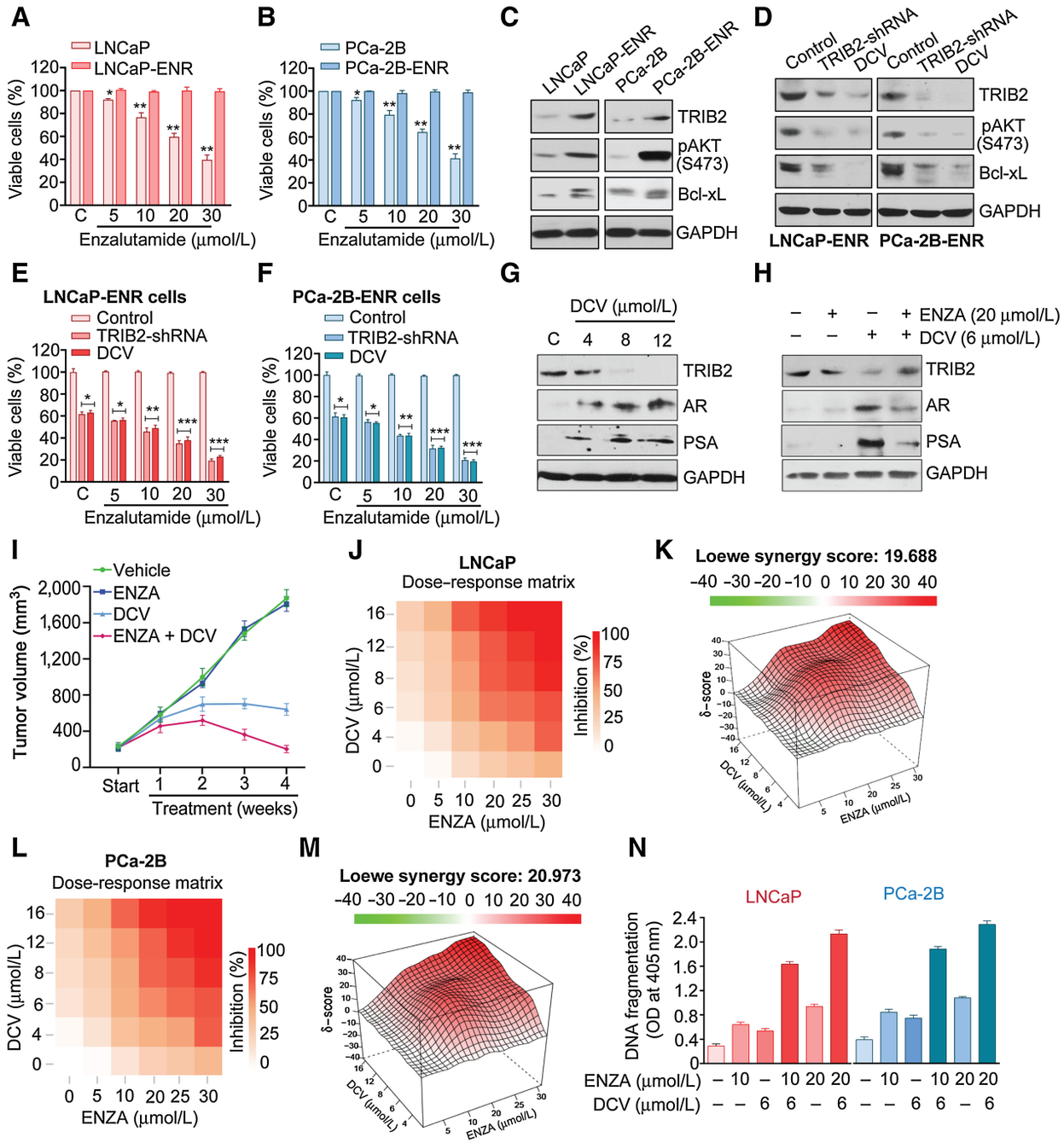

Figure 6.

Resensitization of ERPC cells by DCV. **A** and **B,** Parental (LNCaP, MDA-PCa-2B) and enzalutamide-resistant (LNCaP-ENR, MDA-PCa-2B-ENR) prostate cancer cells were tested for sensitivity to doses of enzalutamide. **C,** Western blot showing increased protein levels of TRIB2 and targets in enzalutamide-resistant cells, compared with parental cells. **D,** Western blot showing protein levels of TRIB2 and targets in TRIB2 shRNA or DCV (6 μmol/L) treated enzalutamide-resistant cells. **E** and **F,** Enzalutamide-resistant (LNCaP-ENR, PCa-2B-ENR) cells were treated with DCV (6 μmol/L) with or without enzalutamide. In another set of experiments, shRNA was used to downregulate TRIB2 in place of DCV. Cell viability was measured by MTS/PES assays. Note: Inhibition of TRIB2 with DCV (6 μmol/L) or lentiviral TRIB2 shRNA (1:10) resensitizes resistant cells to enzalutamide. **G** and **H,** Western blots showing protein levels of TRIB2 and AR signaling proteins in LNCaP-ENR cells. **I,** LNCaP-ENR cells (3×10^6 per mouse) were injected subcutaneously, and mice were treated with vehicle, ENZA (30 mg/kg/day), DCV (30 mg/kg/day), or their combination for 4 weeks via once daily oral gavage ($n = 4$). Tumor size and mice body weights were measured once per week. **J–M,** Synergistic effects of DCV and enzalutamide to inhibit the viability of prostate cancer cells was measured by MTS/PES Assay. The 3D synergy landscape generated by Loewe model show synergistic effects of DCV and ENZA in indicated cells. Cell viability was measured by MTS/PES assay. Note: Red surfaces denote a synergistic interaction and green surfaces an antagonistic interaction. **N,** Prostate cancer cells were treated with enzalutamide, DCV, or combination for 24 hours and apoptotic effects were measured by DNA degradation assay. Data presented as mean values ± SEM. *, $P < 0.05$; **, $P < 0.005$.

Authors' Disclosures

J. Monga reports a patent for Yes pending. C. Hwang reports other support from Johnson & Johnson; grants and personal fees from Merck; grants from Bausch Health, Genentech, Bayer, AstraZeneca; personal fees from TEMPUS, Genzyme, EMD Sorono, OncLive/MJH Life Sciences; and personal fees from Dava Oncology outside the submitted work. S. Gadgeel reports personal fees from Pfizer, Genentech/Roche, AstraZeneca, Mirati, BMS, Blueprint, Merck, Esai, Novartis; and personal fees from Takeda outside the submitted work. J. Ghosh reports a patent for Yes pending and licensed to Filamon. No disclosures were reported by the other author.

Authors' Contributions

J. Monga: Conceptualization, data curation, formal analysis, supervision, validation, investigation, visualization, methodology, writing–review and editing. **F. Valeriote:** Supervision, investigation, visualization, methodology. **C. Hwang:** Supervision, validation, visualization. **S. Gadgeel:** Resources, supervision, funding acquisition, visualization. **J. Ghosh:** Conceptualization, resources, data curation, software, formal analysis, supervision, funding acquisition, validation, investigation, visualization, methodology, writing–original draft, project administration, writing–review and editing.

Acknowledgments

This work was supported by the Henry Ford Health System Research Grants (A10203 and J80024) and by the Dykstra Foundation Grant (F60587) to J. Ghosh.

We acknowledge the help and cooperation from Dr. Patrick Eyers (University of Liverpool, UK) for sending us the 6x His-tagged TRIB2 plasmids and proteins. The authors deeply acknowledge the help and support from the Dykstra Foundation for this study.

The publication costs of this article were defrayed in part by the payment of publication fees. Therefore, and solely to indicate this fact, this article is hereby marked "advertisement" in accordance with 18 USC section 1734.

Note

Supplementary data for this article are available at Molecular Cancer Therapeutics Online (http://mct.aacrjournals.org/).

Received December 12, 2021; revised May 9, 2022; accepted January 6, 2023; published first January 11, 2023.

References

1. Siegel RL, Miller KD, Fuchs HE, Jemal A. Cancer statistics, 2021. CA Cancer J Clin 2021;71:7–33.
2. Tagawa ST, Ramaswamy K, Huang A, Mardekian J, Schultz NM, Wang L, et al. Survival outcomes in patients with chemotherapy-naïve metastatic castration-resistant prostate cancer treated with enzalutamide or abiraterone acetate. Prostate Cancer Prostatic Dis 2021;24:1032–40.
3. Brasso K, Thomsen FB, Schrader AJ, Schmid SC, Lorente D, Retz M, et al. Enzalutamide antitumor activity against metastatic castration-resistant prostate cancer previously treated with docetaxel and abiraterone: A multicenter analysis. Eur Urol 2015;68:317–24.
4. Beer TM, Armstrong AJ, Rathkopf DE, Loriot Y, Sternberg CN, Higano CS, et al. Enzalutamide in metastatic prostate cancer before chemotherapy. N Engl J Med 2014;371:424–33.
5. Penson DF, Armstrong AJ, Concepcion R, Agarwal N, Olsson C, Karsh L, et al. Enzalutamide versus bicalutamide in castration-resistant prostate cancer: The STRIVE trial. J Clin Oncol 2016;34:2098–106.
6. Scher HI, Fizazi K, Saad F, Taplin M, Sternberg CN, Miller K, et al. Increased survival with enzalutamide in prostate cancer after chemotherapy. N Engl J Med 2012;367:1187–97.
7. Shore ND, Chowdhury S, Villers A, Klotz L, Siemens DR, Phung D, et al. Efficacy and safety of enzalutamide versus bicalutamide for patients with metastatic prostate cancer (TERRAIN): a randomized, double-blind, phase II study. Lancet Oncol 2016;17:2153–63.
8. Merseburger AS, Haas GP, von Klot CA. An update on enzalutamide in the treatment of prostate cancer. Ther Adv Urol 2015;7:9–21.
9. Toren P, Kim S, Cordonnier T, Claire-Crafter C, Davies BR, Fazli L, et al. Combination of AZD5363 with enzalutamide significantly delays enzalutamide-resistant prostate cancer in preclinical models. Eur Urol 2015;67:986–90.
10. Tucci T, Zichi C, Buttigliero C, Vignani F, Scagliotti G, Maio M. Enzalutamide-resistant castration-resistant prostate cancer: challenges and solutions. Onco Targets Ther 2018;11:7353–68.
11. Monga J, Subramani S, Bharathan A, Ghosh J. Pharmacological and genetic targeting of 5-lipoxygenase interrupts c-Myc oncogenic signaling and kills enzalutamide-resistant prostate cancer cells via apoptosis. Sci Rep 2020;10:6649.
12. Gibbons JA, Ouatas T, Krauwinkel W, Ohtsu Y, van der Walt JS, et al. Clinical pharacokinetic studies of enzalutamide. Clin Pharmacokinet 2015;54:1043–55.
13. Gibbons JA, de Vries M, Krauwinkel W, Ohtsu Y, Noukens J, van der Walt JS et al. Pharmacokinetic drug interaction studies with enzalutamide. Clin Pharmacokinet 2015;54:1057–69.
14. Monga J, Adrianto I, Rogers C, Gadgeel S, Chitale D, Alumkal JJ, et al. Tribbles 2 pseudokinase confers enzalutamide resistance in prostate cancer by promoting lineage plasticity. J Biol Chem 2022;298:101556.
15. Mata J, Curado S, Ephrussi A, Rørth P. Tribbles coordinates mitosis and morphogenesis in *Drosophila* by regulating string/CDC25 proteolysis. Cell 2000;101:511–22.
16. Foulkes DM, Byrne DP, Yeung W, Shrestha S, Bailey FP, Ferries S, et al. Covalent inhibitors of EGFR family protein kinases induce degradation of human Tribbles 2 (TRIB2) pseudokinase in cancer cells. Sci Signal 2018;11:eaat7951.
17. Keeshan K, He Y, Wouters BJ, Shestova O, Xu L, Sai H, et al. Tribbles homolog 2 inactivates C/EBPalpha and causes acute myelogenous leukemia. Cancer Cell 2006;10:401–11.
18. Eyers PA, Keeshan K, Kannan N. Tribbles in the 21st century: The evolving roles of Tribbles pseudokinases in biology and disease. Trends Cell Biol 2017;27:284–98.
19. Hill R, Madureira PA, Ferreira B, Baptista I, Machado S, Colaço L et al. TRIB2 confers resistance to anticancer therapy by activating the serine/threonine protein kinase AKT. Nat Commun 2017;8:14687.
20. O'Connor C, Yalla K, Salomé M, Moka HA, Gómez Castañeda, Eyers PA et al. Trib2 expression in granulocyte-monocyte progenitors drives a highly drug resistant acute myeloid leukemia linked to elevated Bcl2. Oncotarget 2018;9:14977–92.
21. Zanella F, Renner O, García B, Callejas S, Dopazo A, Carnero A, et al. Human TRIB2 is a repressor of FOXO that contributes to the malignant phenotype of melanoma cells. Oncogene 2010;29:2973–82.
22. Grandinetti KB, Stevens TA, Ha S, Salamone RJ, Walker JR, Zhang J, et al. Overexpression of TRIB2 in human lung cancers contributes to tumorigenesis through downregulation of C/EBPalpha. Oncogene 2011;30:3328–35.
23. Fang Y, Zekiy AO, Ghaedrahmati F, Timoshin A, Farzaneh M, Anbiyaiee A, et al. Tribbles homolog 2 (Trib2), a pseudo serine/threonine kinase in tumorigenesis and stem cell fate decisions. Cell Commun Signal 2021;19:41–6.
24. Mayoral-Varo V, Jiménez L, Link W. The critical role of TRIB2 in cancer and therapy resistance. Cancers 2021;13:2701.
25. Lee C. Daclatasvir: potential role in hepatitis C. Drug Des Devel Ther. 2013;7:1223–33.
26. Sulkowski MS, Gardiner DF, Rodriguez-Torres M, Reddy KR, Hassanein T, Jacobson I, et al. Daclatasvir plus sofosbuvir for previously treated or untreated chronic HCV infection. N Engl J Med 2014;370:211–21.
27. Manns M, Pol S, Jacobson IM, Marcellin P, Gordon SC, Peng CY, et al. All-oral daclatasvir plus asunaprevir for hepatitis C virus genotype 1b: a multinational, phase III, multicohort study. Lancet 2014;384:1597–605.
28. Wyles DL, Ruane PJ, Sulkowski MS, Dieterich D, Luetkemeyer A, Morgan TR, et al. Daclatasvir plus sofosbuvir for HCV in patients coinfected with HIV-1. N Engl J Med 2015;373:714–25.
29. Pol S, Corouge M, Vallet-Pichard A. Daclatasvir–sofosbuvir combination therapy with or without ribavirin for hepatitis C virus infection: from the clinical trials to real life. Hepat Med 2016;8:21–26.
30. Montgomery M, Ho N, Chung E, Marzella N. Daclatasvir (Daklinza): a treatment option for chronic Hepatitis C infection. P T 2016;41:751–5.
31. Ghosh J, Myers CE. Inhibition of arachidonate 5-lipoxygenase triggers massive apoptosis in human prostate cancer cells. Proc Natl Acad Sci USA 1998;95:13182–7.
32. Sarveswaran S, Ghosh R, Morisetty S, Ghosh J. MK591, a second-generation leukotriene biosynthesis inhibitor, prevents invasion and induces apoptosis in the bone-invading C4–2B human prostate cancer cells: implications for the treatment of castration-resistant, bone-metastatic prostate cancer. PLoS One 2015;10:1–19.

33. Ghosh J, Myers CE. Arachidonic acid stimulates prostate cancer cell growth: critical role of 5-lipoxygenase. Biochem Biophys Res Commun 1997;235:418–23.
34. Sarveswaran S, Chakraborty D, Chitale D, Sears R, Ghosh J. Inhibition of 5-Lipoxygenase selectively triggers disruption of c-Myc signaling in prostate cancer cells. J Biol Chem 2015;290:4994–506.
35. Sarveswaran S, Morisetty S, Varma R, Ghosh J. Inhibition of 5-lipoxygenase downregulates stemness and induces apoptosis in prostate cancer stem cells via activation of c-Jun N-terminal Kinase. Oncotarget 2019;10:424–36.
36. Ianevski A, Giri AK, Aittokallio T. SynergyFinder 2.0: visual analytics of multidrug combination synergies. Nucleic Acids Res 2020;48:W488–93.
37. Belema M, Nguyen VN, Bachand C, Deon DH, Goodrich JT, James CA, et al. Hepatitis C virus NS5A replication complex inhibitors: the discovery of daclatasvir. J Med Chem 2014;57:2013–32.
38. Guedj J, Dahari H, Rong L, Sansone ND, Nettles RE, Cotler SJ, et al. Modeling shows that the NS5A inhibitor daclatasvir has two modes of action and yields a shorter estimate of the hepatitis C virus half-life. Proc Natl Acad Sci USA 2013;110:3991–6.
39. Smith MA, Regal RE, Mohammad RA. Daclatasvir: a NS5A replication complex inhibitor for hepatitis C infection. Ann Pharmacother 2016;50:39–46.
40. Berger C, Romero-Brey I, Radujkovic D, Terreux R, Zayas M, Paul D, et al. Daclatasvir-like inhibitors of NS5A block early biogenesis of hepatitis C virus—induced membranous replication factories, independent of RNA replication. Gastroenterology 2014;147:1094–105.
41. Nettles JH, Stanton RA, Broyde J, Amblard F, Zhang H, Zhou L, et al. Asymmetric binding to NS5A by daclatasvir (BMS-790052) and analogs suggests two novel modes of HCV inhibition. J Med Chem 2014;57:10031–43.
42. Nelson DR, Cooper JN, Lalezari JP, Lawitz E, Pockros PJ, Gitlin N, et al. All-oral 12-week treatment with daclatasvir plus sofosbuvir in patients with hepatitis C virus genotype 3 infection: ALLY-3 phase III study. Hepatology 2015;61:1127–35.
43. Daklinza Patient Information has been approved by the U.S. Food and Drug Administration (FDA) [1344554A4]. Full prescribing information for DAKLINZA. DAKLINZA (daclatasvir) tablets, for oral use Initial U.S. Approval: 2015. Available from: https://packageinserts.bms.com/pi/pi_daklinza.pdf.
44. Bunchorntavakul C, Reddy KR. Review article: the efficacy and safety of daclatasvir in the treatment of chronic hepatitis C virus infection. Aliment Pharmacol Ther 2015;42:258–72.
45. Li W, Zhao W, Liu X, Huang X, Lopez OD, Leet JE, et al. Biotransformation of daclatasvir *in vitro* and in nonclinical species: formation of the main metabolite by pyrrolidine δ-oxidation and rearrangement. Drug Metab Dispos 2016;44:809–20.
46. Gamal N, Gitto S, Andreone P. Efficacy and safety of daclatasvir in Hepatitis C: an overview. J. Clin. Transl. Hepatol 2016;4:336–44.
47. Gandhi Y, Eley T, Fura A, Li W, Bertz RJ, GT. Daclatasvir a review of preclinical and clinical pharmacokinetics. Clin Pharmacokinet 2018;57:911–28.

AUTHOR QUERIES

AUTHOR PLEASE ANSWER ALL QUERIES

Q1: Page: 1: Author: Per journal style, genes, alleles, loci, and oncogenes are italicized; proteins are roman. Please check throughout to see that the words are styled correctly. AACR journals have developed explicit instructions about reporting results from experiments involving the use of animal models as well as the use of approved gene and protein nomenclature at their first mention in the manuscript. Please review the instructions at http://aacrjournals.org/content/authors/editorial-policies#genenomen to ensure that your article is in compliance. If your article is not in compliance, please make the appropriate changes in your proof.

Q2: Page: 1: Author: Please verify the drug names and their dosages used in the article.

Q3: Page: 1: Author: Please verify the corresponding author details.

Q4: Page: 2: Author: Units of measurement have been changed here and elsewhere in the text from "M" to "mol/L," and related units, such as "mmol/L" and "μmol/L," in figures, legends, and tables in accordance with journal style, derived from the Council of Science Editors Manual for Authors, Editors, and Publishers and the Système international d'unités. Please note if these changes are not acceptable or appropriate in this instance.

Q5: Page: 4: Author: Please confirm quality/labeling of all images included within this article. Thank you.

Q6: Page: 11: Author: The Authors' Disclosures statement that appears in the proof incorporates the information from forms completed and signed off on by each individual author. No factual changes can be made to disclosure information at the proof stage. However, typographical errors or misspelling of author names should be noted on the proof and will be corrected before publication. Please note if any such errors need to be corrected. Is the disclosure statement correct?

Q7: Page: 11: Author: The contribution(s) of each author are listed in the proof under the heading "Authors' Contributions." These contributions are derived from forms completed and signed off on by each individual author. If you make changes to these contributions, you must inform the affected author(s).

AU: Below is a summary of the name segmentation for the authors according to our records. The First Name and the Surname data will be provided to PubMed when the article is indexed for searching. Please check each name carefully and verify that the First Name and Surname are correct. If a name is not segmented correctly, please write the correct First Name and Surname on this page and return it with your proofs. If no changes are made to this list, we will assume that the names are segmented correctly, and the names will be indexed as is by PubMed and other indexing services.

First Name	**Surname**
Jitender	Monga
Frederick	Valeriote
Clara	Hwang
Shirish	Gadgeel
Jagadananda	Ghosh